

Induced Circular Dichroism Spectrum of α -Cyclodextrin Complex with Heptylviologen

Masato KODAKA* and Toshio FUKAYA

National Chemical Laboratory for Industry, Higashi, Tsukuba 305

(Received October 15, 1988)

The rotational strength of α -cyclodextrin (α -CDx) complex with heptylviologen (1,1'-diheptyl-4,4'-bipyridinium dibromide) was calculated by using the Kirkwood-Tinoco expression. The calculation shows that electric transition polarized along the long axis of heptylviologen gives negative induced circular dichroism (ICD) whereas the short-axis polarized transition gives positive ICD, when HV is axially included in α -CDx and the electric transition moment is located out of the cavity of α -CDx (above the narrower rim). From the comparison between the experimental and calculated results, it is concluded that the heptyl chain of heptylviologen is involved in the cavity while the pyridinium part is situated out of the cavity.

Induced circular dichroism (ICD) has been frequently used to determine the orientation of the aromatic molecule included in α -, β -, and γ -CDx's.¹⁻⁶⁾ The theoretical calculation undertaken thus far is based on the expression developed by Kirkwood and Tinoco, and the agreement between the calculated and experimental results is fairly good.¹⁻⁴⁾

The calculation presented the general rule that the transition with an electric dipole moment parallel to the axis of CDx gives a positive ICD while the transition with an electric dipole moment perpendicular to the axis of CDx gives a negative ICD.¹⁻⁴⁾ Although many experimental data have been analyzed using this rule, we must remember that this rule is applicable only when a chromophore is situated in the cavity of CDx. There has been no calculation dealing with the complex with the chromophore outside the cavity. For example, the complex between α -CDx and heptylviologen (4,4'-diheptyl-1,1'-bipyridinium dibromide; HV) gives negative ICD,⁷⁾ although HV seems to be axially included and the electric transition moment is expected to be parallel to the long axis of HV molecule. The observed ICD spectrum cannot be explained by the general rule described above. In the present study, therefore, the calculation is extended to the outside region of CDx.

Theoretical

The theoretical rotational strength of the transition from the ground state (0) to the excited state (a), R_{0a} , was calculated by the same method as that of Harata et al.,¹⁾ using the following Kirkwood-Tinoco expression.⁸⁾

$$R_{0a} = \pi \nu_a \mu_{0a}^2 \sum_j \frac{\nu_{0j}^2 (\alpha_{33} - \alpha_{11})_j (GF)_j}{c(\nu_{0j}^2 - \nu_a^2)}$$

$$(GF)_j = \frac{1}{r_j^3} \left[\vec{e}_{0a} \cdot \vec{e}_j - \frac{3(\vec{e}_{0a} \cdot \vec{r}_j)(\vec{e}_j \cdot \vec{r}_j)}{r_j^2} \right] \vec{e}_{0a} \times \vec{e}_j \cdot \vec{r}_j$$

Here \vec{e}_j is the unit vector in the direction of the symmetry axis of the bond j in α -CDx; \vec{r}_j is the vector directed from the center of the chromophore (bipyridi-

nium moiety) to the bond j in α -CDx; ν_{0j} is the frequency of the electric transitions of the bond j in α -CDx; \vec{e}_{0a} is the unit vector in the direction of the electric dipole moment (μ_{0a}) of the transition from the ground state (0) to the excited state (a) in the chromo-

Table 1. The Frequency of the Electronic Transitions (ν_0) and Polarizability (α_{33} , α_{11}) of the Bonds in a Glucose Residue

Bond	$\nu_0 \times 10^{-15}/s^{-1}$	$\alpha_{33}/\text{\AA}^3$	$\alpha_{11}/\text{\AA}^3$
C-O	1.67	0.89	0.46
C-C	2.00	0.98	0.27

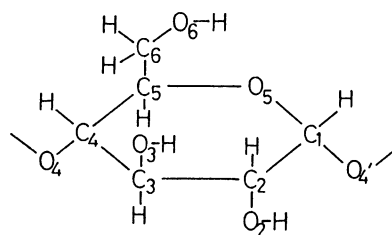
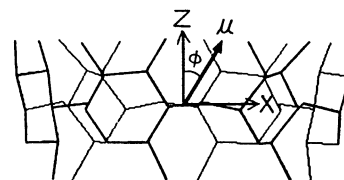
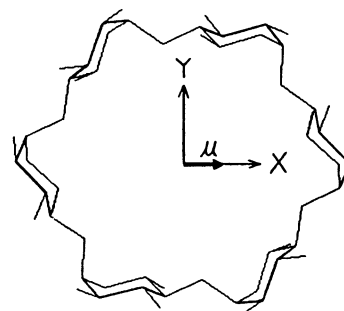


Fig. 1. The schematic drawing of α -CDx.

phore, and ν_a is its frequency; α_{33} and α_{11} are bond polarizability at zero frequency parallel and perpendicular, respectively, to the symmetry axis of the bond in α -CDx; c is the velocity of light.

The values of α_{33} , α_{11} ,^{9,10)} and ν_{0j} ¹¹⁾ are shown in Table 1. The assignment of the electronic transition of HV was undertaken by the CNDO/S-CI calculation. The electric transition moment was put at the center of the bipyridinium moiety. The geometry of α -CDx was derived from the X-ray data of the α -CDx-potassium acetate complex.¹¹⁾ The axes of the coordinates were defined as shown in Fig. 1, where the origin of the coordinates was fixed on the plane determined by the six O₄ atoms. All the C₆-O₆ and O-H bonds were neglected owing to the flexibility. Furthermore, the effects of all the C-H bonds were neglected, for they may have isotropic polarizability.¹²⁾

Results and Discussion

As the angle of twist (θ) around the central C-C bond of HV cannot be determined unequivocally, it seems to be appropriate that the CNDO/S-CI calculation is done at each point corresponding to the planar and angular conformations. In the case of biphenyl, the angle θ is about 42° in the gaseous phase,^{13,14)} while it is planar in the crystalline state.¹⁵⁾ On the other hand, in solution θ is 23°.¹⁶⁾ Taking into account these results about biphenyl, θ of HV is expected to be about 0–45°. And so we have undertaken the MO calculation about the three conformations ($\theta=0^\circ$, 22.5°, and 45°), with the central C-C bond length of HV fixed to 1.48 Å. For the pyridinium rings, all the C-N and C-C bond lengths and all the bond angles were assumed to be similar to those of benzene ring. The other bond lengths and bond angles were estimated from the standard values. In the CI calculations, 60 singly-excited configurations were taken into consideration. In Table 2 are summarized the calculated wavelengths and symmetries of the lower singlet states together with the oscillator strengths. The symmetries were determined on the assumption that HV has D_{2h} conformation for $\phi=0^\circ$ and D₂ conformations for $\phi=22.5^\circ$ and 45°. In the wavelength region under consideration, there can be seen three transitions. In these transitions, the A_g→B_{3u} (or A→B₃) transition has the largest intensity, with its moment directed along the long axis of HV. On the

other hand, the oscillator strength of the A_g→B_{2u} (or A→B₂) transition is only ca. 40% of that of the A_g→B_{3u} (or A→B₃) one, and the A_g→B_{1g} (or A→B₁) transition is negligible as compared with the A_g→B_{3u} (or A→B₃) transition. Experimentally HV has the absorption at 264 nm ($D=38.4$ debye²), while the CNDO/S-CI calculation reproduced reasonable wavelengths and dipole strengths (the A_g→B_{3u} or the A→B₃ transition); $\lambda=266$ nm and $D=51.0$ debye² at $\theta=0^\circ$, $\lambda=261$ nm and $D=48.0$ debye² at $\theta=22.5^\circ$, $\lambda=250$ nm and $D=40.0$ debye² at $\theta=45^\circ$; with the corresponding electric transition moments along the long axis of HV molecule.

In Fig. 2 is shown the dependence of the rotational strength of α -CDx-HV complex on the Z coordinates, with the X and Y coordinates fixed to be 0 Å. The electric transition moment is rotated in the X-Z plane by the angle ϕ as shown in Fig. 1. Inside the cavity of α -CDx, the large positive ICD is given at $\phi=0^\circ$ (maximum; 36.3×10^{-40} cgs at $Z=-0.5$ Å) and the negative ICD at $\phi=90^\circ$ (minimum; -17.7×10^{-40} cgs at $Z=-0.6$ Å). These results agree qualitatively with those for β -CDx complex obtained by Harata et al.¹⁾ On the other hand, outside the cavity the sign of the ICD value is reversed, especially remarkably on the side of the primary hydroxyl groups (narrower rim) of α -CDx, with minimum at $\phi=0^\circ$ (-19.6×10^{-40} cgs at

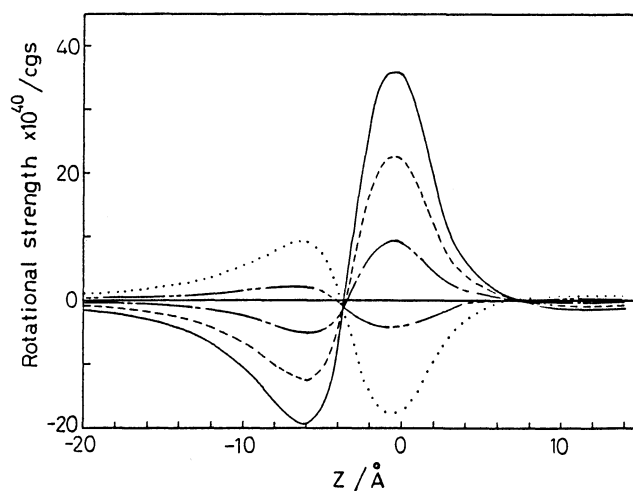


Fig. 2. The dependence of the calculated rotational strengths of α -CDx-HV complex on the Z coordinates ($X=Y=0$ Å). The directions of the electric transition moment (the angle ϕ) are 0° (—), 30° (---), 45° (-·-·-), 60° (— · —), 90° (·····).

Table 2. Calculated Wavelength (λ) and Oscillator Strength (f) of the Electronic Transitions of Heptylviologen

Type	$\theta=0^\circ$		Type	$\theta=22.5^\circ$		Type	$\theta=45^\circ$	
	λ	f		λ	f		λ	f
	nm			nm			nm	
A _g →B _{1g}	294	0.00	A→B ₁	290	0.02	A→B ₂	280	0.29
A _g →B _{2u}	286	0.36	A→B ₂	285	0.34	A→B ₁	279	0.06
A _g →B _{3u}	266	0.90	A→B ₃	261	0.87	A→B ₃	250	0.75

$Z = -6.1 \text{ \AA}$) and maximum at $\phi = 90^\circ$ (9.2×10^{-40} cgs at $Z = -6.4 \text{ \AA}$). As shown in the previous report, methylviologen (1,1'-dimethyl-4,4'-bipyridinium dichloride) does not give ICD, while HV with hydrophobic alkyl chains gives negative ICD ($R = -5.7 \times 10^{-40}$ cgs) at 257 nm. It is suggested that in the case of HV the heptyl chain is included in the cavity of α -CDx and the bipyridinium part is placed outside the cavity.⁷⁾ This speculation is compatible with the calculated results shown in Fig. 2. Although there is a possibility that the $A_g \rightarrow B_{2u}$ (or $A \rightarrow B_2$) transition with the short-axis polarization may contribute to the positive rotational strength, the value must be about five times smaller than that due to the $A_g \rightarrow B_{3u}$ (or $A \rightarrow B_3$) transition in view of the results shown in Table 2 and Fig. 2. Consequently, the contribution from the $A_g \rightarrow B_{2u}$ (or $A \rightarrow B_2$) transition seems to be negligible.

Figures 3–5 show the rotational strength calculated with moving the position of the electric transition moment of HV in the X-Y plane, concerning the nar-

rower rim region of α -CDx ($Z \leq -4 \text{ \AA}$). In these figures, the left-hand figures indicate the rotational strength maps for the α -CDx-HV complex at various ϕ values. The maps are drawn on the rectangular region containing the X and Y-axes, the electric transition moment being parallel to the X-Z plane with a given rotation angle ϕ . The right-hand figures in Figs. 3–5 show the approximate negative ICD region (black region). When $Z = -4.0 \text{ \AA}$ and $\phi = 0^\circ$ (Fig. 3 (a)), the negative region (black) is located in the centre of the map while the positive area (white) is far from the centre. As ϕ increases, the negative region shifts to the surroundings (Fig. 3 (b), (c)) and at last the central area becomes positive at $\phi = 90^\circ$ (Fig. 3 (d)). Similar tendencies are found in the case of $Z = -6.0 \text{ \AA}$ and $Z = -8.0 \text{ \AA}$ (Figs. 4 and 5). The rotational strength maps for $Z = -6.0 \text{ \AA}$ and $Z = -8.0 \text{ \AA}$ are relatively simple and resemble each other, whereas those for $Z = -4.0 \text{ \AA}$ is more complicated (Fig. 3). Although the distribution of the positive area varies with the Z and ϕ values, it can be estimated qualitatively from Figs. 3–5 that the long axis of HV is nearly parallel to the axis of α -CDx, probably $0 \leq \phi < \text{ca. } 30^\circ$, and the centre of HV is not so

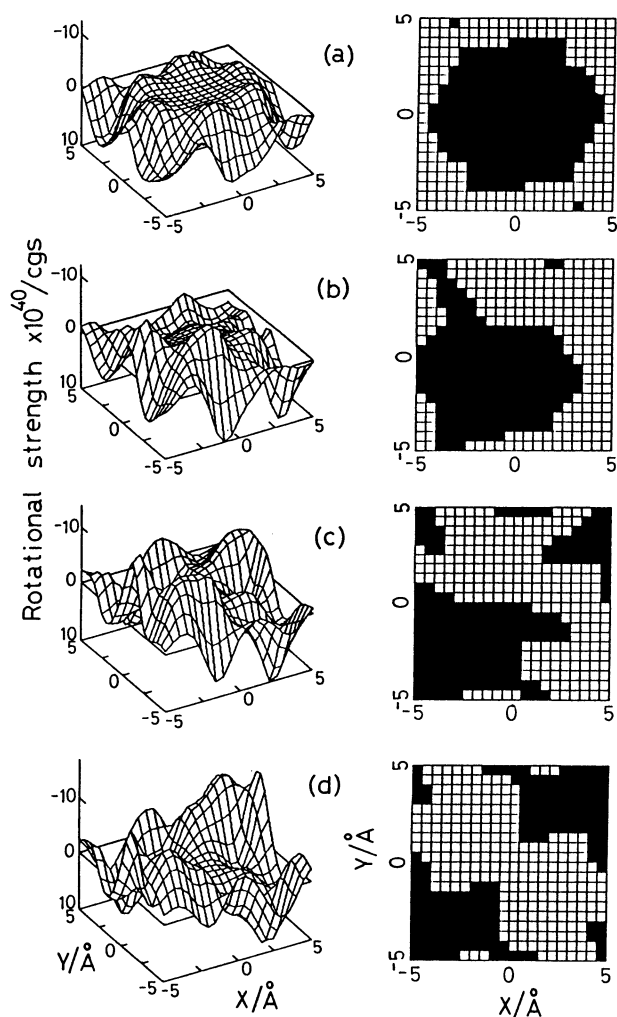


Fig. 3. The rotational strength maps for the α -CDx-HV complex at $Z = -4.0 \text{ \AA}$. (a) $\phi = 0^\circ$, (b) $\phi = 30^\circ$, (c) $\phi = 60^\circ$, (d) $\phi = 90^\circ$. The black area of the right-hand figures shows the approximate negative ICD region.

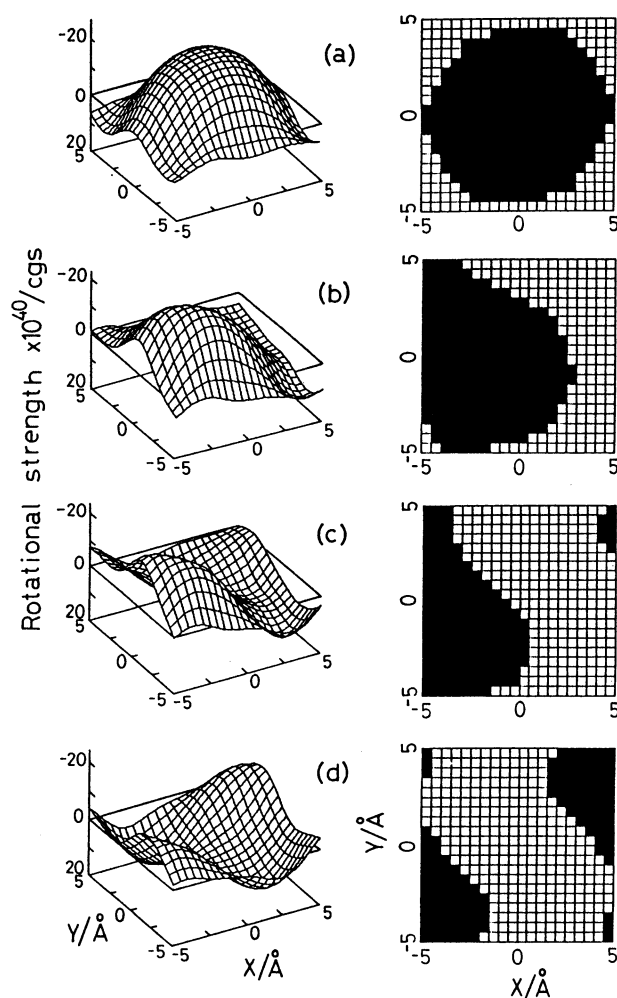


Fig. 4. Same as Fig. 3; $Z = -6.0 \text{ \AA}$.

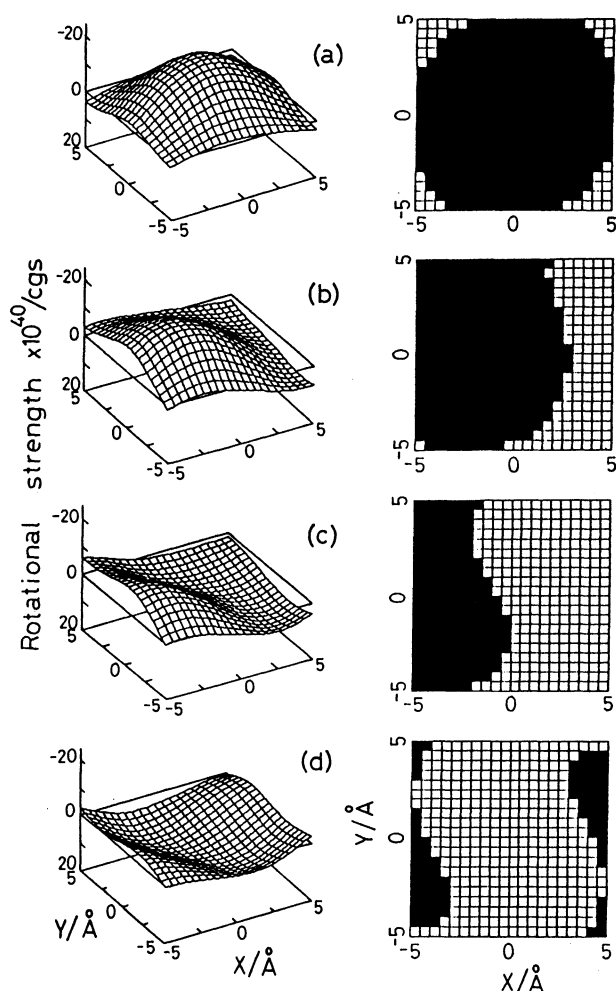


Fig. 5. Same as Fig. 3; $Z = -8.0 \text{ \AA}$.

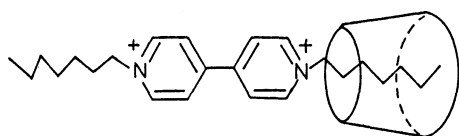


Fig. 6. The schematic drawing of α -CDx-HV complex.

far from the axis of α -CDx, perhaps within 4–5 \AA .

From the calculation undertaken in the present study, it can be said qualitatively that when a chromophore is placed outside the cavity of CDx (especially above the narrower rim), the transition with an electric dipole moment nearly parallel to the axis of CDx gives a negative ICD and the transition with perpendicular polarization gives a positive ICD. This rule is quite

the reverse of the general rule presented by Harata et al. for the chromophore included in the inner region of β -CDx.¹⁾ The estimated structure of the α -CDx-HV complex is schematically depicted in Fig. 6.

Recently CDx derivatives which bear aromatic groups bound to the primary hydroxyl groups (narrower rim) have been studied by using CD spectra, as models of host-guest phenomena.^{17–20)} The findings obtained in the present study may be also useful for analyzing such CDx derivatives.

The authors wish to thank Dr. Kazutoshi Tanabe, National Chemical Laboratory for Industry, for his kind supply of the CNDO/S-CI program.

References

- 1) K. Harata and H. Uedaira, *Bull. Chem. Soc. Jpn.*, **48**, 375 (1975).
- 2) H. Shimizu, A. Kaito, and M. Hatano, *Bull. Chem. Soc. Jpn.*, **52**, 2678 (1979).
- 3) H. Shimizu, A. Kaito, and M. Hatano, *Bull. Chem. Soc. Jpn.*, **54**, 513 (1981).
- 4) H. Shimizu, A. Kaito, and M. Hatano, *J. Am. Chem. Soc.*, **104**, 7059 (1982).
- 5) N. Kobayashi, *J. Chem. Soc., Chem. Commun.*, **1988**, 918.
- 6) H. Yamaguchi, M. Higashi, and M. Oda, *Spectrochim. Acta*, **44A**, 547 (1988).
- 7) M. Kodaka and T. Fukaya, *Bull. Chem. Soc. Jpn.*, **59**, 2032 (1986).
- 8) I. Tinoco, Jr., *Adv. Chem. Phys.*, **4**, 113 (1962).
- 9) C. G. Le Fèvre and R. J. W. Le Fèvre, *J. Chem. Soc.*, **1956**, 3549.
- 10) R. J. W. Le Fèvre, A. Sundaram, and R. K. Pierens, *J. Chem. Soc.*, **1963**, 479.
- 11) A. Hybl, R. E. Rundle, and D. E. Williams, *J. Am. Chem. Soc.*, **87**, 2779 (1965).
- 12) C. G. Le Fèvre and R. J. W. Le Fèvre, *Chem. Ind.*, **1955**, 1121.
- 13) O. Bastiansen and M. Treatterberg, *Tetrahedron*, **17**, 147 (1962).
- 14) A. Almenningen and O. Bastiansen, *K. Nor. Vidensk. Selsk. Skr.*, **1958**, 4.
- 15) J. Trotter, *Acta Crystallogr.*, **14**, 1135 (1961).
- 16) H. Suzuki, *Bull. Chem. Soc. Jpn.*, **32**, 1350 (1959).
- 17) A. Ueno, I. Suzuki, and T. Osa, *Chem. Pharm. Bull.*, **35**, 2151 (1987).
- 18) A. Ueno, F. Moriwaki, T. Osa, F. Hamada, and K. Murai, *Chem. Pharm. Bull.*, **34**, 438 (1986).
- 19) A. Ueno, F. Moriwaki, T. Matsue, and T. Osa, *Makromol. Chem., Rapid Commun.*, **6**, 231 (1985).
- 20) A. Ueno, F. Moriwaki, T. Osa, F. Hamada, and K. Murai, *J. Am. Chem. Soc.*, **110**, 4323 (1988).